The Influence of the Madden–Julian Oscillation on Precipitation in Oregon and Washington*

NICHOLAS A. BOND AND GABRIEL A. VECCHI

NOAA/Pacific Marine Environmental Laboratory, and University of Washington/Joint Institute for the Study of the Atmosphere and Ocean, Seattle, Washington

(Manuscript received 13 August 2002, in final form 16 January 2003)

ABSTRACT

The Madden–Julian oscillation (MJO) is the primary mode of large-scale intraseasonal variability in the Tropics. Previous work has explored the influences of the MJO on atmospheric circulation anomalies over the North Pacific Ocean and precipitation in California, among other effects. This study focuses on the relationship between the MJO and mean precipitation in the states of Oregon and Washington and that between the MJO and the occurrence of flooding in western Washington. The MJO is diagnosed using principal component analysis of 850-hPa zonal winds from the NCEP–NCAR reanalysis for 1979–2000. The dataset for precipitation is daily rain gauge data gridded on a scale of 50 km and covering 1979–94. The occurrence of flooding is based on streamflow records from the Sauk, Snoqualmie, and Chehalis Rivers for 1979–2000. The results indicate that the phase of the MJO has a substantial systematic effect on intraseasonal variability in precipitation in Oregon and Washington in both early winter (October–December) and late winter (January–March). The MJO is also associated with a statistically significant enhancement and modulation of floods in early winter. The phases of the MJO that promote enhanced precipitation in the mean and increased incidence of western Washington floods are substantially different during early winter than during late winter. It is suggested that this result is attributable to the difference in the atmospheric circulation of the North Pacific in early versus late winter.

1. Introduction

There is a temporal gap in the forecasting of precipitation in the Pacific Northwest (and other locations). On timescales of less than a week or two, relatively deterministic predictions are formed using output from numerical weather prediction (NWP) model simulations. On timescales from about a month to a year, the projections are more statistical in nature and are based on slowly evolving elements of the atmosphere–ocean system, notably El Niño–Southern Oscillation (ENSO). On intermediate timescales, useful outlooks may be possible through consideration of the effects of the Madden–Julian oscillation (MJO) on the atmospheric circulation over the North Pacific Ocean and western North America (e.g., Higgins and Mo 1997; Waliser et al. 2003).

The MJO is the dominant mode of subseasonal tropospheric variability over the tropical Indian and Pacific Oceans. The MJO was originally identified as a coherent, eastward-propagating perturbation in tropical sea level pressure and upper-level wind with a spectral peak in the 40–50-day band (Madden and Julian 1972). More recent descriptions of the MJO indicate that it includes a range of periods, generally between 30 and 90 days. The MJO has received much attention because of its influence on many aspects of tropical weather, including deep cumulus convection (e.g., Madden and Julian 1972, 1994; Rui and Wang 1990; Hendon and Salby 1994) and tropical cyclone activity (e.g., Liebmann et al. 1994; Maloney and Hartmann 2000a,b). The characteristic near-equatorial MJO signal in atmospheric convection and low-level divergent flow propagates eastward at an average speed of approximately 5 m s^{-1} over the Indian Ocean and western equatorial Pacific; in the Western Hemisphere the MJO is associated with a tropospheric wind perturbation that propagates eastward at approximately 10 m s^{-1} (Hendon and Salby 1994).

The dynamical processes that cause the MJO remain incompletely understood. A central issue relates to whether the MJO results from purely atmospheric processes or whether it represents a coupled ocean–atmosphere mode of variability (e.g., Hendon and Glick 1997; Wang and Xie 1998; Shinoda et al. 1998; Harrison and Vecchi 2001). There is increasing evidence that the MJO is an instability that includes tropical–extratropical

* NOAA/Pacific Marine Environmental Laboratory Contribution Number 2479 and Joint Institute for the Study of the Atmosphere and Ocean Contribution Number 934.

Corresponding author address: Nicholas A. Bond, NOAA/PMEL, 7600 Sand Point Way NE, Seattle, WA 98115-6349.
E-mail: nickolas.a.bond@noaa.gov

coupling (e.g., Frederiksen 2002 and references therein). At any rate, most coupled ocean–atmosphere models are unable to produce a realistic MJO to this day, and predictions of the MJO over multiple cycles remain elusive. Nevertheless, there is potential skill in MJO forecasts out to a few weeks through extrapolation from current conditions.

The impact of the MJO on the atmospheric circulation outside of the Tropics has been of considerable interest. There is evidence that deep tropical convection forces the midlatitude flow both directly (e.g., Hoskins and Karoly 1981; Horel and Wallace 1981) and indirectly (e.g., Schubert and Park 1991). The indirect forcing is through deep convection's effects on the zonal wind in the tropical upper troposphere, which in turn affects the propagation of waves originating in midlatitudes. The consequence of these interactions is systematic relationships between tropical convection with the MJO and extratropical wave trains (e.g., Lau and Phillips 1986). Of direct relevance to this study, Higgins and Mo (1997) illustrated the effects of the variability in tropical Pacific convection associated with the MJO (as defined in terms of outgoing longwave radiation, or OLR) on the flow over the North Pacific, and Higgins et al. (2000) and Mo and Higgins (1998) described the relationships between tropical convection and U.S. West Coast precipitation. The latter study had a broad perspective, considering the winter (December–March) as a whole and West Coast precipitation more on a regional rather than a local basis. Because the mean atmospheric circulation over the North Pacific evolves over the course of the cooler half of the year, the linkages between the MJO and Pacific Northwest precipitation are also likely to vary. In addition, a different type of synoptic situation promotes heavy precipitation west of the Cascade Mountains of Oregon and Washington State versus east of the Cascades; the MJO's impact on those regions is liable to be more robust when one considers them in isolation rather than in combination.

The purpose of this study is to examine further the impacts of tropical variability associated with the MJO on cool-season precipitation in the Pacific Northwest. In essence, we seek to bridge the gap between the climate perspective provided by Higgins, Mo, and others and the event-scale perspective provided in the study of heavy (and warm) rains over western Washington by Lackmann and Gyakum (1999). We diagnose the state of the MJO, and the corresponding anomalies in the atmospheric circulation over the North Pacific and North America, using the National Centers for Environmental Prediction–National Center for Atmospheric Research (NCEP–NCAR) reanalysis dataset for the period of 1979–2000. We consider the effects of the MJO early in the cool season (October–December) separate from that late in the cool season (January–March). We illustrate the spatial patterns of precipitation associated with the MJO using a dataset of daily precipitation on a 50-km grid (Widmann and Bretherton 2000). In addition, we describe the relationship between the MJO and extreme precipitation events, that is, floods, using streamflow records from selected western Washington rivers. This component of the study is motivated by our observation that the synoptic conditions associated with heavy precipitation in a mean sense are not necessarily identical to those associated with western Washington floods. A notable recent example here is the winter of 1998–99, which represented the wettest on record in portions of western Washington but lacked any major floods.

2. Datasets

We make use of a variety of datasets. For diagnosis of the MJO, and for determining its relationship to the circulation over the North Pacific and western North America, we use the 850-hPa zonal winds and 500-hPa heights, respectively, from the NCEP–NCAR extended reanalysis product [Kalnay et al. (1996); the datasets were available online from the National Oceanic and Atmospheric Administration (NOAA)–Cooperative Institute for Research in Environmental Sciences (CIRES) Climate Diagnostics Center (CDC) at http://www.cdc.noaa.gov/]. As a proxy for atmospheric deep convection in the Tropics, we use a global $2.5^\circ \times 2.5^\circ$ daily gridded OLR dataset as described by Liebmann and Smith (1996) (provided by NOAA–CIRES CDC; it also was available online at http://www.cdc.noaa.gov/). Because satellite data are consistently available to constrain the 850-hPa wind fields in the Tropics only since 1979, we consider the period of 1979–2000.

The precipitation over Washington and Oregon is specified using the dataset described by Widmann and Bretherton (2000). This dataset consists of daily values on a 50-km grid and is based on rain gauge data, with account taken for topographical effects by using the Precipitation–Elevation Regressions on Independent Slopes Model (PRISM). The scheme used by Widmann and Bretherton (2000) appears to be suited well for describing both the temporal and spatial variability in a region of complex orography such as the Pacific Northwest. The period of record available here is 1979–94.

For each of the datasets described above, we generate a monthly climatic dataset by averaging. These monthly means were interpolated to daily values that were then subtracted to form anomalies for each parameter.

The relationship(s) between the MJO and flooding in western Washington are investigated using streamflow observations from the Sauk River near Sauk, the Snoqualmie River at Carnation, and the Chehalis River near Grand Mound. These data are from U.S. Geological Service gauges (D. McDonnal, National Weather Service Forecast Office, Seattle, Washington, 2002, personal communication). These three rivers were picked to represent the hydrological conditions in the north,

central, and southern portions, respectively, of the west flank of the Cascade Mountains of Washington. Their locations are shown later (Fig. 2). We consider only the major events, that is, floods with magnitudes corresponding to a 2-yr return period and greater. The period of record used here is 1979–2000.

3. MJO identification and composites

We diagnose the MJO using an index based on intraseasonal near-equatorial 850-hPa zonal wind variability. Shinoda et al. (1998) used essentially the same technique, but with an OLR-based index. Our procedure is based on the observations that the MJO represents the dominant mode of large-scale, intraseasonal, near-equatorial tropospheric wind variability and that it features an eastward propagation. The input wind data are available daily, on a global 2.5° × 2.5° grid. The 850-hPa zonal winds are intraseasonally filtered for periods between 35 and 120 days and are averaged between 5°S and 5°N to produce an intraseasonal, near-equatorial 850-hPa zonal wind dataset ($U850'_{eq}$).

Empirical orthogonal function (EOF) analysis is applied to the $U850'_{eq}$ dataset; the first two EOFs describe an eastward-propagating mode in $U850'_{eq}$. These two EOFs explain 34% and 18% of the variance. We define an amplitude A and phase Φ based on the time series from the first two EOFs:

$$A(t) = [\langle \mathrm{PC}_1(t)\rangle^2 + \langle \mathrm{PC}_2(t)\rangle^2]^{1/2} \quad \text{and}$$

$$\Phi(t) = \tan^{-1}[\langle \mathrm{PC}_1(t)\rangle/\langle \mathrm{PC}_2(t)\rangle],$$

where the brackets $\langle\ \rangle$ indicate a 20-day boxcar time smoothing. Using these quantities, we define an MJO event as a period of 30 or more days during which A exceeds 0.7 standard deviation and during which the phase is moving in an eastward direction for the entire period. The periods found ranged from about 40 to 90 days. The MJO is active, as defined above, 61% of the time in October–December (OND) and 68% of the time in January–March (JFM). As a test of our results, MJO events were also defined based on days on which A exceeds 1 standard deviation. The results in this case included stronger signals in Pacific Northwest precipitation, with nearly identical spatial and temporal patterns. We chose to use the 0.7 threshold for A to incorporate more days/events in our analysis. The phase of the MJO is determined by the angle of Φ and is divided into eight parts ($-\pi \geq \Phi > -3/4\pi \Rightarrow$ phase 1, $-3/4\pi \geq \Phi > -\pi/2 \Rightarrow$ phase 2, etc.). Time series of the MJO amplitude and phase used in our analysis were available online (http://ferret.pmel.noaa.gov/mjo/servlets/dataset) at the time of writing.

To illustrate the structure and evolution of the tropical wind and convective signal associated with the MJO, the composite (all season) MJO 850-hPa zonal wind and OLR anomalies are shown in Fig. 1. Note the difference in eastward propagation speeds over the ''warm pool'' waters of the Indian and west Pacific Oceans versus over the central and eastern Pacific and note also the asymmetry of the convective and wind signals. Westerly (easterly) wind anomalies tend to lead reduced (enhanced) convection. The structure of the MJO composite from our definition describes the principal characteristics of the MJO in convection and winds (see Madden and Julian 1972, 1994; Rui and Wang 1993) and is similar to that based on other indices (e.g., Hendon and Salby 1994; Maloney and Hartmann 1998).

We generate composites of precipitation-rate anomalies with respect to the MJO by averaging the various parameters for each of the eight phases. Separate composites are constructed for OND and JFM. Given the period of record and that the MJO is active roughly two-thirds of the time, about 130 days of data are available for composites of the precipitation in Oregon and Washington in each phase. About 180 days of data are available for composites of 500-hPa heights over the North Pacific and western North America, and 850-hPa zonal winds and OLR in the tropical Pacific, in each phase of the MJO. We explore the relationships between floods in western Washington and the MJO in a different fashion. We consider each flood event separately and determine whether it occurred during an active period of the MJO and, if so, at which phase. As for the precipitation composites, the floods during OND and JFM are treated separately.

Two kinds of tests are made: one for the ''MJO modulation'' of precipitation and floods, and one for the ''MJO enhancement'' of precipitation and floods. MJO modulation means that the timing of mean precipitation rate anomalies or floods with respect to MJO phase is significantly different from that associated with a uniform distribution. MJO enhancement means that the mean precipitation rates or the frequency of floods is significantly different during active versus inactive periods of the MJO. If the latter is the case, then there is statistical evidence for the enhancement, or suppression, of precipitation or flooding by the MJO.

The technique used to evaluate the statistical significance of our results is outlined here. Because precipitation anomalies are not normally distributed, to test for statistical significance we used a bootstrap method (Efron and Tibshirani 1991), incorporating 100 000 bootstrap samples. The bootstrap method involves randomly sampling the record to determine the distribution of precipitation anomalies during days of a particular phase of the MJO relative to those in all other days, at each location. On the maps presented in the following section, the mean values of precipitation anomalies for each phase of the MJO are plotted where their values are statistically significant at the 95% level. This method is similar to that used by Vecchi and Harrison (2000) to examine the sea surface temperature changes following wind variability in the tropical Pacific and by Vecchi

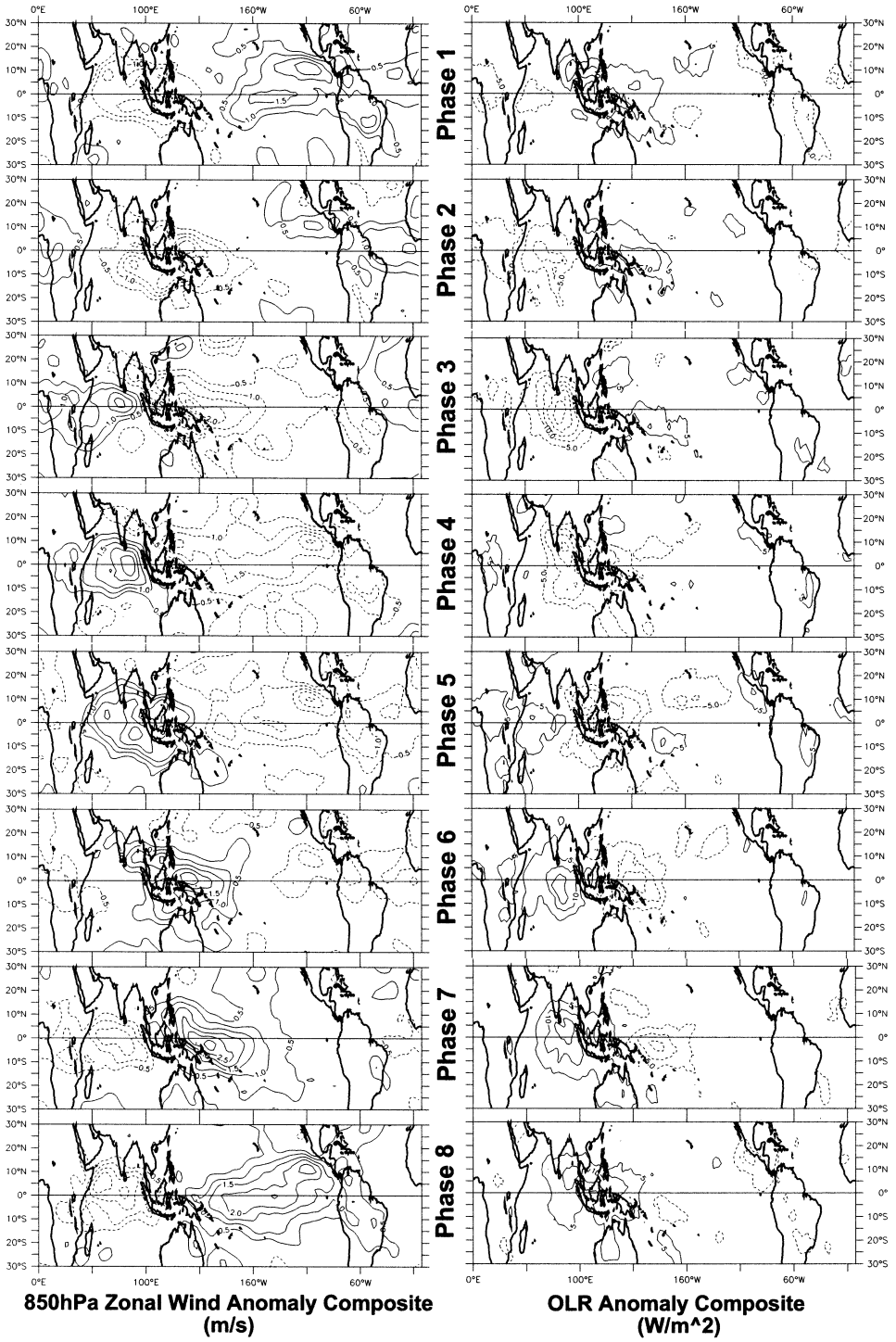

FIG. 1. Composite (left) 850-hPa zonal wind anomalies and (right) OLR anomalies panels during active periods of the MJO. Solid (dashed) contours represent positive (negative) anomalies with intervals of 0.5 m s^{-1} for the 850-hPa zonal wind and 5 W m^{-2} for the OLR. See text for details on the definition of the phase of the MJO.

(2000) to examine the structure of MJO convection and surface winds.

With regard to floods, we perform two distinct tests, one for MJO modulation of flooding events and the other for MJO enhancement of flooding events. The statistical significance of MJO modulation of flooding events is determined by finding the sets of phases for which the number of flooding events is significantly different from a binomial distribution, with probability given by

$$1 - \sum_{N=i}^{j} p(\text{phase}N).$$

We adjust for our a posteriori hypothesis development based on the possible number of ways the phases could have been chosen; for example, there are eight possible ways to choose two adjacent phases. We also determine whether a flooding event is likelier to occur when an MJO is present than when it is not, that is, whether there is MJO enhancement of flooding events. We do this by examining whether the number of flooding events occurring when the MJO is absent is significantly different from a binomial distribution, with probability given by

$$1 - p(\text{MJO}).$$

This method is adapted from that used by Vecchi (2000) to explore statistical relationships between tropical Pacific westerly wind events and the MJO.

4. Results

As context for the results that follow, we first present maps of the mean precipitation over Washington and Oregon for the OND and JFM periods (Fig. 2). Roughly 4 times as much precipitation falls on the west side versus the east side of the Cascades Mountains of Oregon and Washington. In an overall sense, very similar precipitation amounts occur in OND as in JFM. There is a small tendency for the precipitation to be greater in OND than in JFM in the northern portion of the domain.

The mean atmospheric circulation in OND and JFM is summarized in terms of the 200-hPa vector wind fields (Fig. 3). Note that the mean upper-tropospheric jet across the Pacific is weaker and its core is located farther north, especially near the western coast of North America, in OND than in JFM. Perturbations in the upper-level jet across the northeast Pacific are therefore liable to have different impacts in OND than in JFM on the weather (including precipitation) along the U.S. West Coast.

Precipitation rate anomalies during OND in Oregon and Washington as a function of MJO phase are shown in Fig. 4. The maps are masked to show values only where anomalies are statistically significant at the 95% confidence level. Relatively wet conditions occur during MJO phases 7 and 8, and dry conditions occur during

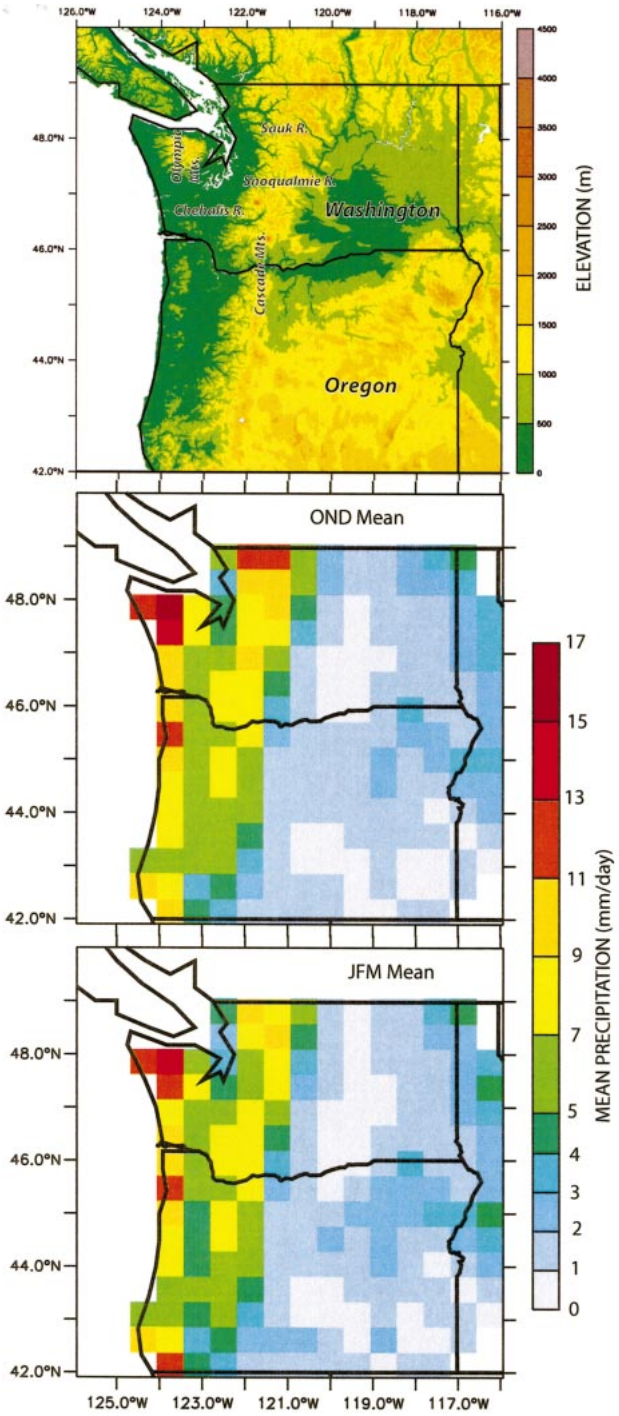

FIG. 2. (top) Topography and river locations. Mean precipitation rates (mm day^{-1}) during (middle) OND and (bottom) JFM for 1979–94. Gradations are at 1 mm day^{-1} (2 mm day^{-1}) at precipitation rates of less (more) than 5 mm day^{-1}.

MJO phases 1, 2, and 4. The precipitation anomalies tend to be much more pronounced on the west side than on the east of the Cascade Mountains. The magnitudes of the dry anomalies at their peak (phase 2) are typically

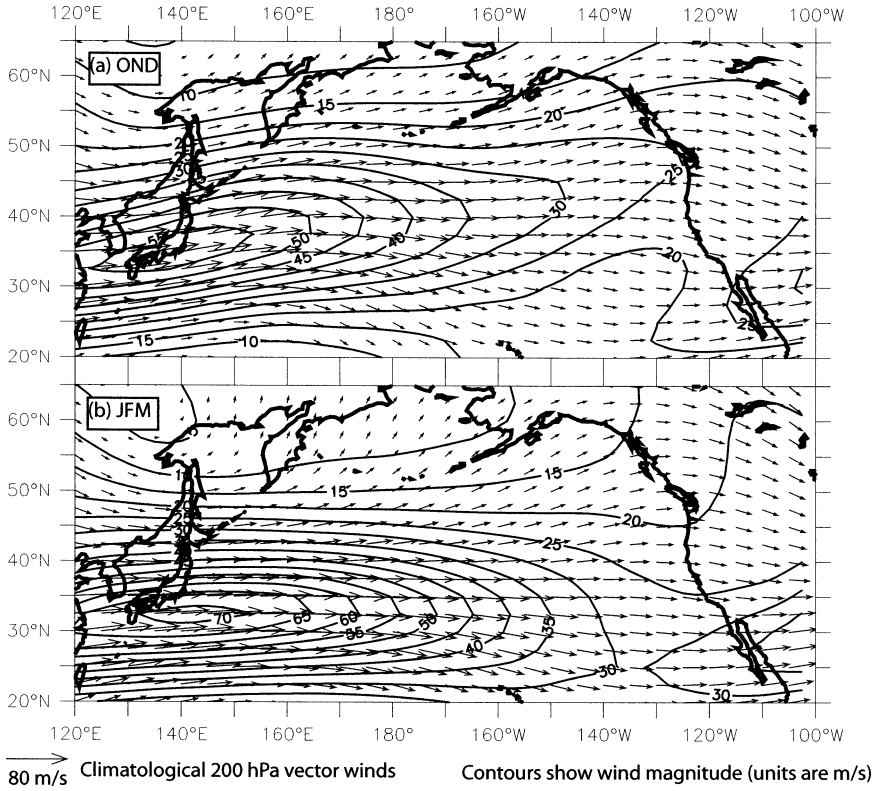

FIG. 3. Mean 200-hPa vector winds (m s^{-1}) during (a) OND and (b) JFM 1979–2000 from the NCEP–NCAR reanalysis dataset.

2–5 mm day^{-1}, which represents a reduction of roughly 20%–40% from the mean precipitation rates. The peak wet anomalies (during phases 7 and 8) are typically 3–5 mm day^{-1} and as much as 9 mm day^{-1}, which represents an enhancement of roughly 30%–>50% from the mean precipitation rates. In other words, the precipitation west of the Cascades during phase 8 ranges from 150% to more than 200% of that during phase 2. East of the Cascades, the peak precipitation anomalies are also on the order of 30%–40% of the mean rates, but the areal coverage of statistically significant anomalies is less. The tropical 850-hPa zonal wind and OLR composites associated with the MJO (Fig. 1) indicate that, during OND, Oregon and Washington tend to be wet when the MJO cycle features peak westerly wind anomalies near the date line and suppressed deep convection over the eastern Indian Ocean and Indonesia. Oregon and Washington tend to be dry when the core of the easterly wind anomalies with the MJO is located between the east Indian Ocean and the central Pacific. It is interesting that transitions in precipitation rates accompanying the MJO can be rapid (e.g., between phases 6 and 7).

Precipitation rate anomalies during JFM in Oregon and Washington as a function of MJO phase, the late-season counterparts to Fig. 4, are shown in Fig. 5. A decidedly different phasing is found as compared with that for OND. During JFM, precipitation is favored during phase 5 of the MJO (a phase in which precipitation anomalies are weak during OND) and is suppressed significantly during phases 2 and 7. The magnitudes of these anomalies are comparable to the peak anomalies during OND. It turns out that the MJO was in phase 5 during 17–18 January 1986, the specific event detailed by Lackmann and Gyakum (1999). The magnitude of the MJO signal in JFM relative to that in OND is comparable in western Washington and is weaker in western Oregon. The wet phase of the MJO for the Pacific Northwest in JFM (phase 5) corresponds to the portion of the MJO cycle in which westerly wind anomalies are present just west of Indonesia and enhanced deep convection occurs over Indonesia.

We also explored the difference between the mean precipitation rates during the roughly 2/3 of the days on which the MJO is active from the remaining days on which it is inactive (i.e., MJO enhancement). In OND, the MJO is associated with enhanced precipitation in western Washington and with reduced precipitation in eastern Oregon and extreme southwestern Idaho. The magnitude of this signal (the difference between the precipitation rates in active vs inactive periods of the MJO) ranges from 1 to 2.5 mm day^{-1} in the Olympic Mountains and from 0.5 to 1 mm day^{-1} in Puget Sound and the western Cascade Mountains.

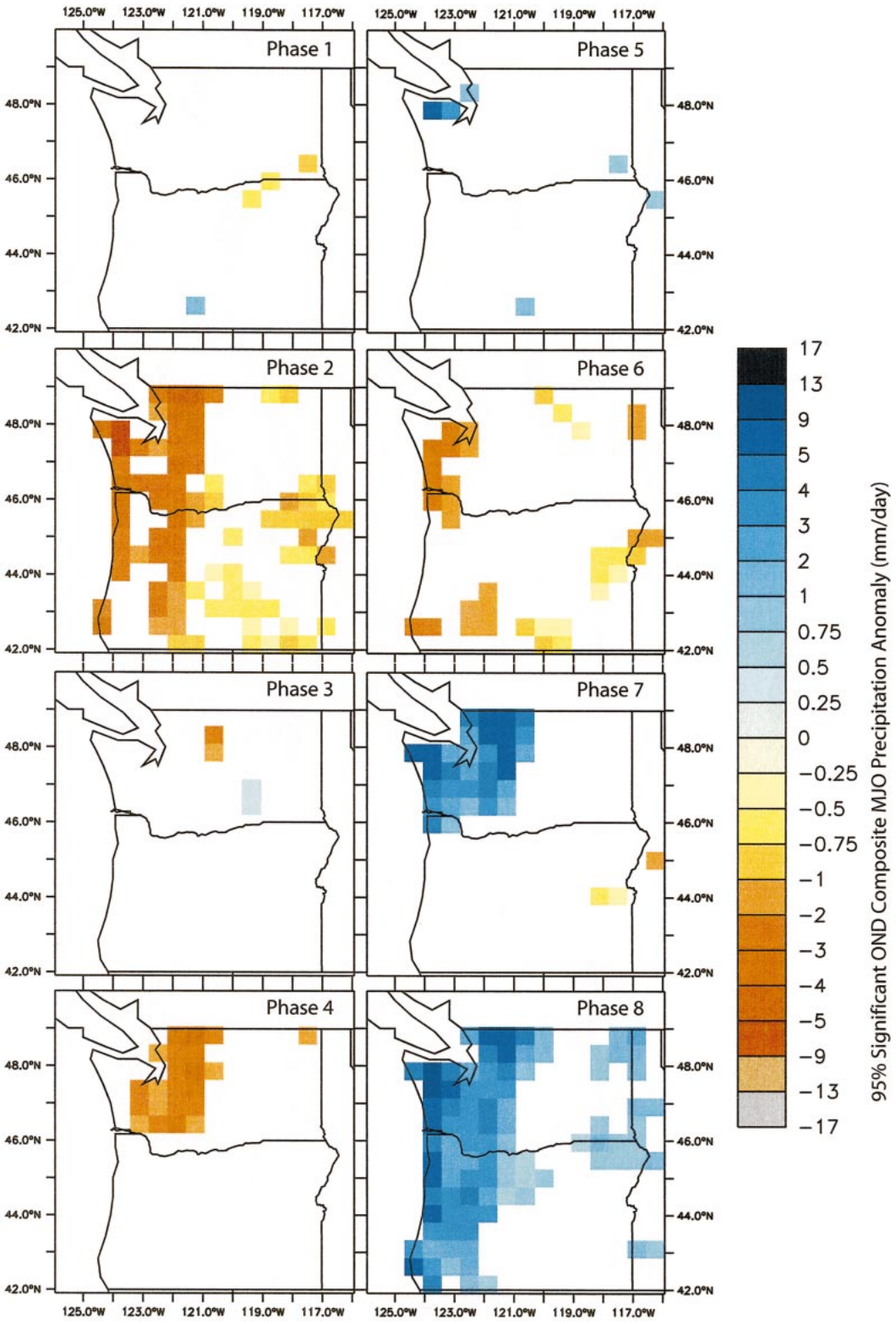

FIG. 4. Composite precipitation rate anomalies (mm day^{-1}) vs MJO phase during OND for 1979–94. Gradations are at 0.25 mm day^{-1} (1 mm day^{-1}) for precipitation rate anomalies of magnitudes less (more) than 1 mm day^{-1}. White areas indicate where the signal is statistically insignificant at the 95% confidence level.

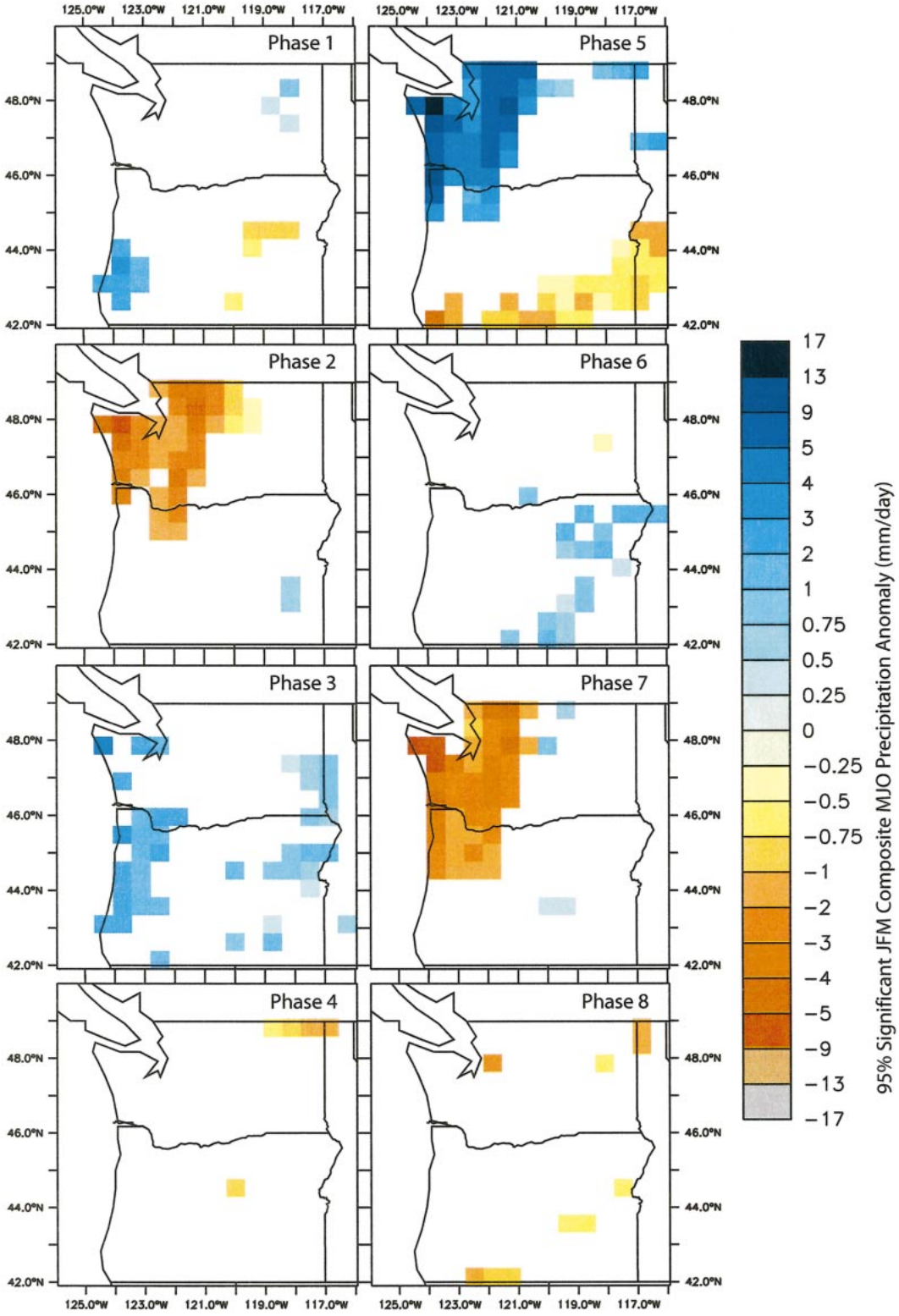

FIG. 5. As in Fig. 4 but for JFM.

The magnitudes of the reductions in precipitation are more modest, with values generally less than 0.5 mm day^{-1}. In JFM, the principal signals are net enhancement of precipitation in southern coastal Oregon, with values less than 1 mm day^{-1}, and net reduction of precipitation in the Cascade Mountains in Washington, with values between 0.5 and 1 mm day^{-1}. In an overall sense, the MJO enhancement is weaker than the MJO modulation of precipitation, but the former is still significant in selected locations at the 90% confidence level.

It is interesting to compare the MJO's influence on mean precipitation with its influence on flooding. Here we restrict ourselves to western Washington, in part because the MJO signal on mean precipitation is strong and because we had access to long records of streamflow for that region. We expect that the three selected rivers adequately represent hydrological conditions in western Washington because floods in western Washington are caused by synoptic-scale disturbances (Lackmann and Gyakum 1999) rather than smaller-scale convective storms. Most of the floods considered here occurred on at least two of the three rivers at the same time.

The results with regard to the MJO and western Washington floods in OND and JFM are shown in Figs. 6a and 6b, respectively. We use polar plots to illustrate the distributions of individual events, showing both their magnitudes in terms of streamflow relative to the historical peak flow and their timing with respect to the phase of the MJO. A strong relationship between the MJO and floods is found for OND (Fig. 6a). Fully one-half of the 32 total floods occurred during just one-eighth of the MJO cycle (phase 7). Zero floods occurred during one-quarter of the MJO cycle (phases 1 and 2). The distribution shown in Fig. 6a is evidence for MJO modulation of floods on each river, with statistical significance at the 99% level. The phasing of floods versus the MJO is similar but not identical to its counterpart involving mean precipitation. The most notable difference is that the flooding tends to occur more often in phase 7 but the mean precipitation is greater in phase 8. One other difference is that there were slightly fewer flood events but greater mean precipitation in MJO phase 5 than in phases 4 and 6. We found that 7 out of 8 floods on the Chehalis, 11 out of 14 floods on the Snoqualmie, and 13 out of 20 floods on the Sauk occurred during active periods of the MJO in OND. Because the MJO during OND is active 61% of the time, these results indicate evidence for MJO enhancement of flooding on the Chehalis and Snoqualmie Rivers (with statistical significance at the 95% and 90% levels, respectively) but no evidence for MJO enhancement of flooding on the Sauk River.

The relationship between the MJO and floods in JFM (Fig. 6b) is apparently weaker than that during OND. In part this may be due to the smaller incidence of floods (one-half that during OND) and hence a less

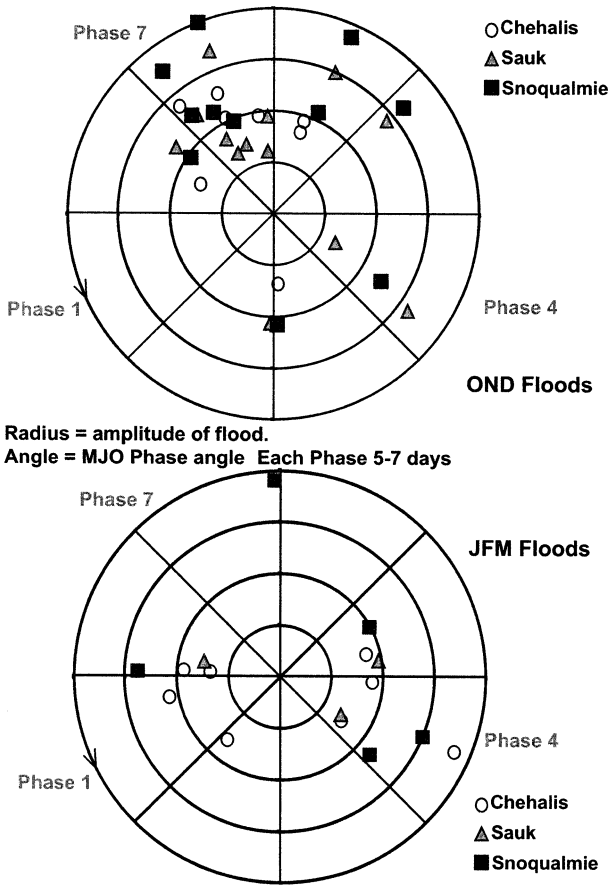

FIG. 6. Polar diagrams of floods on the Sauk, Snoqualmie, and Chehalis Rivers during (a) OND and (b) JFM for 1979–2000. The magnitudes of these floods in terms of streamflow are proportional to radius (the outer ring represents the all-time record peak flow on each river); the timing of these floods with respect to the phase of the MJO is shown by the azimuth (see labels on the perimeter of each diagram). Only flood events with a 2-yr return period and greater are included.

statistically reliable dataset. There is a small preference for floods in JFM during MJO phases 4 and 5, during which the mean precipitation is near normal and enhanced, respectively. Aside from the one event on the Snoqualmie River, there appears to be suppression of floods during MJO phases 6 and 7, during which the mean precipitation was near normal and substantially below normal, respectively. There is also a cluster of JFM floods during MJO phases 8–2, however, during which the mean precipitation is below normal in an overall sense. We note that all the floods in the latter cluster occurred from mid-February through March, whereas all the floods in the cluster for MJO phases 4 and 5 occurred from January just into February. Because just a handful of events are involved here, we feel that it is imprudent to attribute too much to this distinction. In terms of the statistical reliability of MJO modulation of floods in JFM, the binomial test (considering JFM on the whole) reveals that none of the

three rivers exhibits distributions different from a uniform distribution at confidence levels exceeding 85%. A longer record length would help to establish the relationships between the MJO and floods in JFM. With regard to MJO enhancement of floods in JFM, we found only weak and inconsistent signals (enhancement on the Chehalis, but suppression on the Snoqualmie and Sauk). In summary, the MJO influences the incidence of western Washington floods strongly in OND, but these influences are less defined in JFM.

The MJO affects precipitation in Oregon and Washington through its influences on the planetary-scale atmospheric circulation in the Northern Hemisphere. Here we illustrate that the circulation anomalies accompanying the MJO are significantly different in OND than in JFM. The anomalous circulation is characterized through composite 500-hPa geopotential height anomaly maps as a function of MJO phase for OND (Fig. 7) and JFM (Fig. 8). In general, all of the principal height anomaly centers were found to be statistically significant at the 90% level, again using the bootstrap method. The results for OND show anomalous 500-hPa ridging over the Pacific Northwest during MJO phases 1 and 2, consistent with anomalously low precipitation. The linkage between the 500-hPa height anomaly pattern and precipitation becomes less straightforward by MJO phase 4, for which anomalous troughing in the northeast Pacific implies enhanced southerly flow (which might be expected to promote precipitation) but at least western Washington tends to be dry. It is presumed that the key here is that, in this phase of the MJO, the synoptic-scale flow is not directed sufficiently onshore. Relatively weak 500-hPa flow anomalies from the northwest are indicated for MJO phases 5 and 6, and, not surprising, these phases include only weak signals in precipitation. The patterns for MJO phases 7 and 8 include prominent troughs in the North Pacific and anomalous 500-hPa flow from the southwest over the Pacific Northwest. This setup is favorable for heavy rain in the Pacific Northwest, as shown by Lackmann and Gyakum (1999), and indeed our precipitation composites (Fig. 4) indicate wet conditions.

There are crucial differences between JFM and OND in the 500-hPa geopotential height anomaly patterns associated with the MJO. For example, in MJO phase 5 there is enhanced westerly 500-hPa flow (and positive precipitation anomalies) in JFM but weak northwesterly flow and minor precipitation anomalies in OND. During MJO phase 7, anomalous troughing off the U.S. West Coast brings about easterly 500-hPa flow anomalies to the Pacific Northwest (Fig. 8) and hence dry conditions in JFM, whereas in OND this trough is enough farther north (Fig. 7) to enhance the precipitation in the Pacific Northwest. In a very broad sense, the 500-hPa anomaly centers over the North Pacific and western North America during JFM tend to be located south and/or east of their corresponding locations during OND. There are exceptions to this relationship; the anomaly patterns in JFM little resemble those in OND during MJO phases 2 and 4. The observed shift in the MJO-induced 500-hPa height anomalies between OND and JFM is plausibly related to the change in the mean atmospheric circulation, in particular the southward migration and eastward extension of the upper-tropospheric jet across the North Pacific (Fig. 3).

5. Discussion

The influence of the MJO on the weather outside of the Tropics has been the subject of earlier study, and it is worthwhile to examine how the current results compare with previous results. In particular, Mo and Higgins (1998) described the North Pacific atmospheric circulation and U.S. West Coast precipitation anomalies associated with the MJO. The precipitation signal that they found for Oregon and Washington (their Fig. 6) ranged from a negative peak of about -0.4 mm day^{-1} to a positive peak of about 1.0 mm day^{-1}. In contrast, we found a much stronger signal, up to almost an order of magnitude greater, in selected locations. This difference can be attributed in part to our use of a newly available precipitation dataset with resolution that is roughly 5 times as great and a better accounting of orographic effects. Some of this difference can also be attributed to the manner of presentation. Mo and Higgins (1998) presented their results in terms of latitudinal bands averaged from 118° to 125°W, whereas we present our results in terms of maps. These maps preserve the longitudinal structure in the precipitation anomalies associated with the MJO—in particular the large values to the west of the Cascade Mountains. Mo and Higgins (1998) also found two longitudes (120°E and 135°W) at which negative OLR anomalies (i.e., enhanced deep convection) correspond to maxima in West Coast precipitation at the latitudes of Oregon and Washington, but this result stems partly from their consideration of the December–March period as a whole. From our analysis, there is a single range of longitudes for which enhanced tropical convection tends to be accompanied by wet conditions in the Pacific Northwest, but this range of longitudes is different in OND than in JFM. Some discrepancies in the two sets of results may stem from differences in definition of the MJO; Mo and Higgins (1998) used OLR, whereas we used 850-hPa zonal winds and restricted ourselves to eastward-propagating perturbations. The latter aspect may also account for some of the differences between Mo and Higgins (1998) and Jones (2000) on the effects of the MJO on precipitation in California. The definitions of the MJO by Jones (2000) were based on eastward-propagating anomalies in OLR and 850-hPa zonal winds; he found a preference for extreme precipitation events when convection was enhanced between 120° and 150°E, whereas Higgins and Mo found greater mean precipitation for California with negative

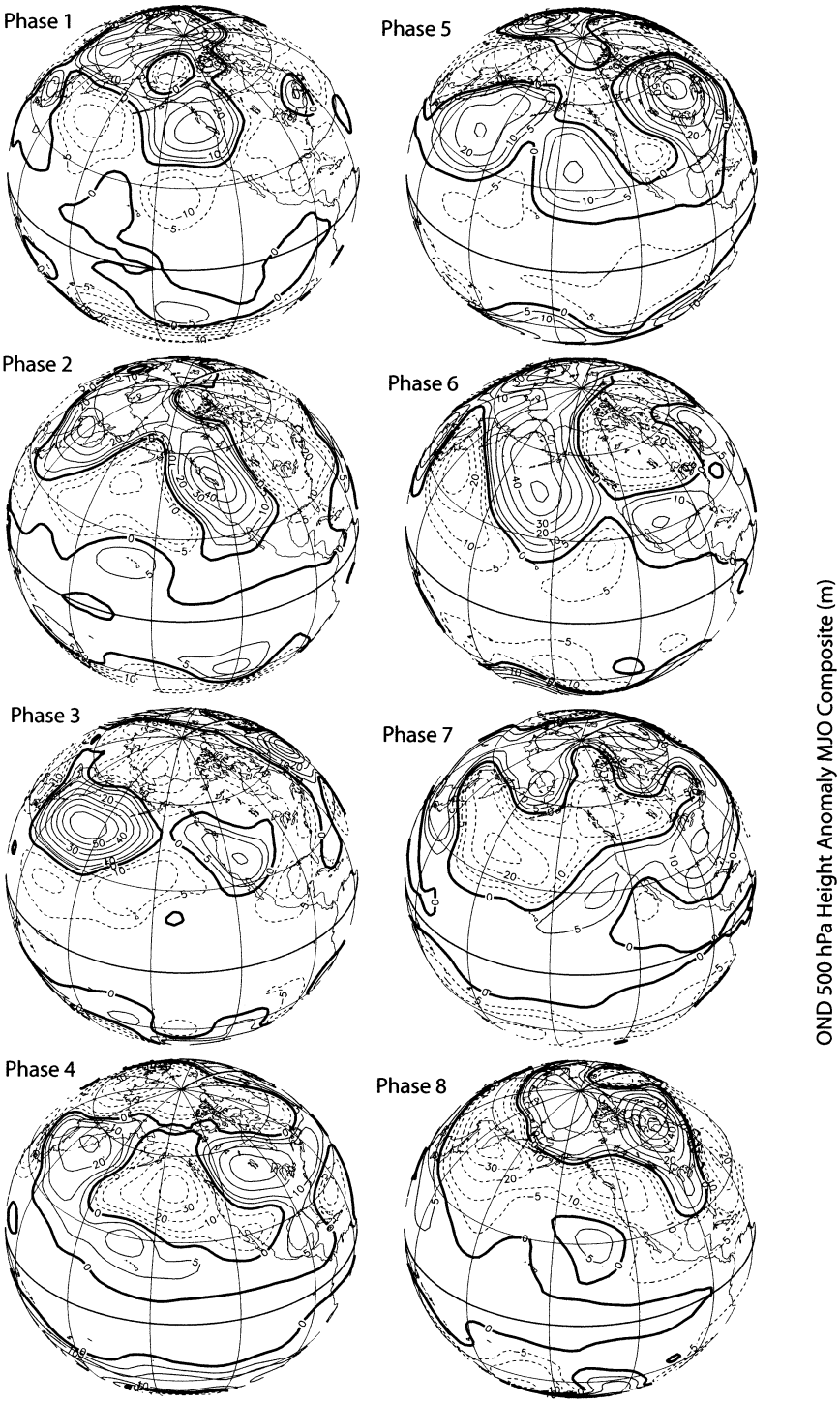

FIG. 7. Composite 500-hPa geopotential height anomalies (m) vs MJO phase during OND for 1979–2001.

OLR anomalies near 135°W. The issue of propagating versus nonpropagating tropical variability is potentially important because this aspect affects the interactions between the Tropics and midlatitudes (e.g., Hoskins and Yang 2000).

Our results appear to be robust, but they are based on a limited sample size and hence are subject to a degree of uncertainty. Two additional caveats bear mentioning. The periods of analysis (from 1979 to 1994 or 2000) included a tendency for more warm

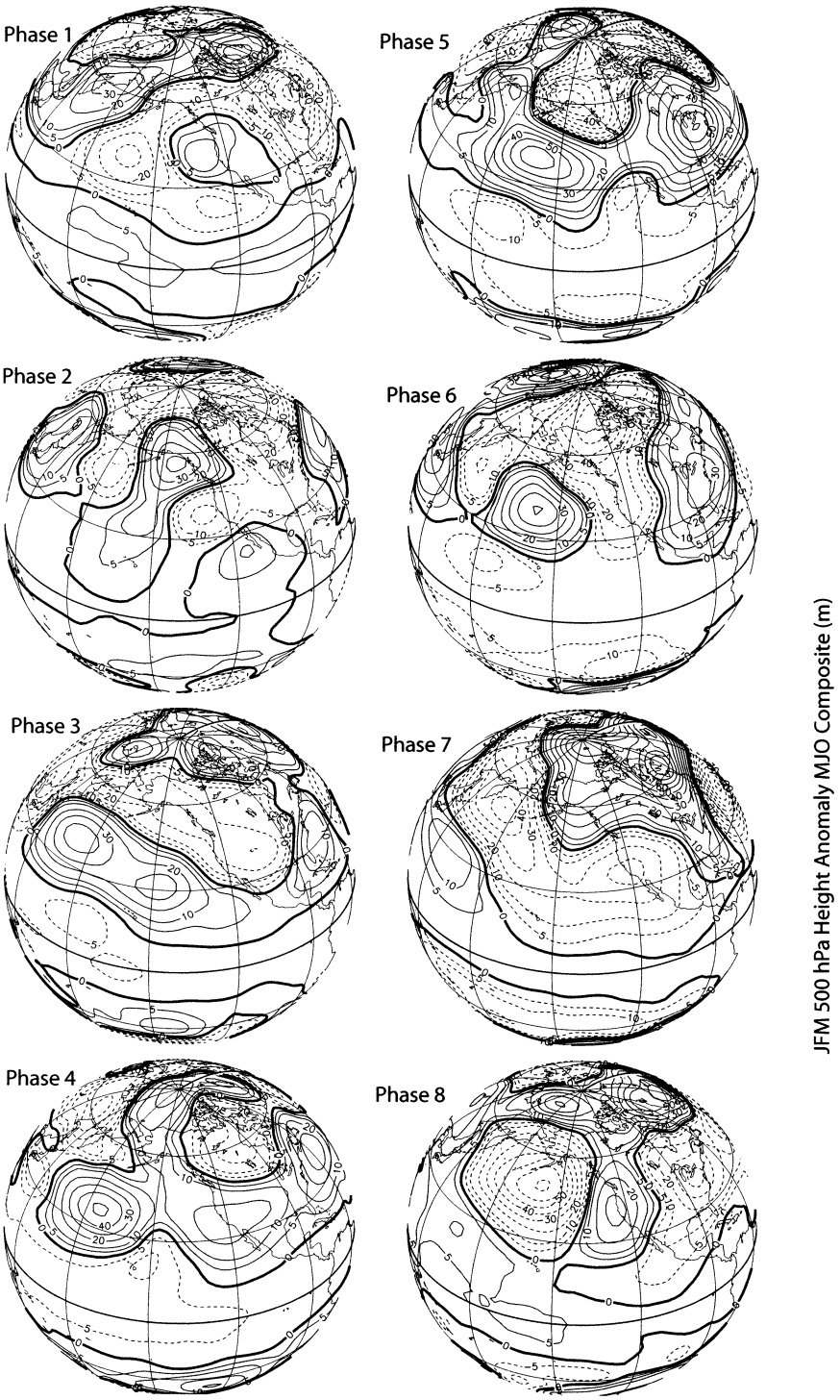

FIG. 8. As in Fig. 7 but for JFM.

ENSO conditions than cold ENSO conditions and for the Pacific decadal oscillation (Mantua et al. 1997) to be in a positive state. It is unknown whether these decadal-scale background conditions influence the response of Pacific Northwest precipitation to the MJO and hence represent an important context for the results found here. Second, our analysis has had the benefit of hindsight in specification of the MJO; that is, it is diagnostic rather than prognostic. To make predictions based on the MJO, the MJO itself needs to be forecast.

To our knowledge, such forecasts are not currently being made in an operational sense. Nevertheless, the MJO is monitored in real time (e.g., http://www.cpc.ncep.noaa.gov/products/intraseasonal/index.html), and it should be possible to make reasonably accurate extrapolations from its current state over at least a fraction of a cycle, especially when it is active. These kinds of extrapolations are being done experimentally using OLR following the technique of Wheeler and Kiladis (1999) and are at this time available online (http://www.bom.gov.au/bmrc/clfor/cfstaff/matw/maproom/OLR_modes/index.htm). It should be feasible to adapt the scheme of Waliser et al. (1999), which consisted of a statistical model for tropical rainfall that is based on the evolution of MJO out to lead times of 20 days, to Pacific Northwest precipitation.

There is a reason why we have focused in this study on precipitation rather than on other elements of Pacific Northwest weather. Our synoptic experience indicates that regional precipitation is more related to the large-scale nature of the circulation anomalies associated with the MJO than are other important cool-season phenomena such as windstorms and lowland snowstorms. These kinds of events tend to be more local, and both their development and impacts depend on details in the flow that are less apt to be related to large-scale disturbances emanating from the Tropics. That being said, because the circulation anomalies associated with the MJO are prominent throughout the North Pacific (Figs. 7 and 8), we expect that there are other kinds of weather phenomena in other regions of the Pacific basin (perhaps arctic-air outbreaks in southern Alaska or cyclogenesis in the Bering Sea, etc.) that are modulated by the MJO.

6. Summary

The MJO has been shown to have a systematic influence on cool-season precipitation in western Oregon and Washington. The magnitude of the MJO-based signal exceeds one-third of the mean precipitation rate in some locations. Resolving this signal required a proper accounting of mesoscale variations in precipitation (both in the mean and as modulated by the MJO) and of the difference in the atmospheric circulation's response to the MJO in OND versus JFM. We suggest that the association between the MJO and Pacific Northwest precipitation west of the Cascade Mountains could be exploited to provide useful outlooks on the 1–3-week timescale.

Acknowledgments. We thank Doug McDonnal at the NWS Forecast Office in Seattle for providing the streamflow observations used in our analysis. We thank D. E. Harrison for encouragement and suggestions. The manuscript benefited from comments by Brant Liebmann and three anonymous reviewers. NAB appreciates the support from the Pan-American Climate Studies (PACS) program of NOAA's Office of Global Programs (OGP). GAV acknowledges support by NOAA (OAR HQ and OGP) through the UW/PMEL Hayes Center and by NASA's physical oceanography program. This publication was supported by the Joint Institute for the Study of the Atmosphere and Ocean (JISAO) under NOAA Cooperative Agreement NA17RJ1232.

REFERENCES

Efron, B., and R. Tibshirani, 1991: Statistical data analysis in the computer age. *Science,* **253,** 390–395.

Frederiksen, J. S., 2002: Genesis of intraseasonal oscillations and equatorial waves. *J. Atmos. Sci.,* **59,** 2761–2781.

Harrison, D. E., and G. A. Vecchi, 2001: January 1999 Indian Ocean cooling event. *Geophys. Res. Lett.,* **28,** 3717–3720.

Hendon, H. H., and M. L. Salby, 1994: The life cycle of the Madden–Julian oscillation. *J. Atmos. Sci.,* **51,** 2225–2237.

——, and J. Glick, 1997: Intraseasonal air–sea interaction in the tropical Indian and Pacific Oceans. *J. Climate,* **10,** 647–661.

Higgins, R. W., and K. C. Mo, 1997: Persistent North Pacific circulation anomalies and the tropical intraseasonal oscillation. *J. Climate,* **10,** 223–244.

——, J.-K. E. Schemm, W. Shi, and A. Leetmaa, 2000: Extreme precipitation events in the western United States related to tropical forcing. *J. Climate,* **13,** 793–820.

Horel, J. H., and J. M. Wallace, 1981: Planetary scale atmospheric phenomenon associated with the Southern Oscillation. *Mon. Wea. Rev.,* **109,** 813–829.

Hoskins, B. J., and D. J. Karoly, 1981: The steady linear response of a spherical atmosphere to thermal and orographic forcing. *J. Atmos. Sci.,* **38,** 1179–1196.

——, and G.-Y. Yang, 2000: The equatorial response to higher-latitude forcing. *J. Atmos. Sci.,* **57,** 1197–1213.

Jones, C., 2000: Occurrence of extreme precipitation events in California and relationships with the Madden–Julian oscillation. *J. Climate,* **13,** 3576–3587.

Kalnay, E., and Coauthors, 1996: The NCEP/NCAR 40-Year Reanalysis Project. *Bull. Amer. Meteor. Soc.,* **77,** 437–471.

Lackmann, G. L., and J. R. Gyakum, 1999: Heavy cold-season precipitation in the northwestern United States: Synoptic climatology and analysis of the flood of 17–18 January 1986. *Wea. Forecasting,* **14,** 687–700.

Lau, K.-M., and T. J. Phillips, 1986: Coherent fluctuations of extratropical geopotential height and tropical convection in intraseasonal time scales. *J. Atmos. Sci.,* **43,** 1164–1181.

Liebmann, B., and C. A. Smith, 1996: Description of a complete (interpolated) outgoing longwave radiation dataset. *Bull. Amer. Meteor. Soc.,* **77,** 1275–1277.

——, H. H. Hendon, and J. D. Glick, 1994: The relationship between tropical cyclones of the western Pacific and Indian Oceans and the Madden–Julian oscillation. *J. Meteor. Soc. Japan,* **72,** 401–411.

Madden, R. A., and P. R. Julian, 1972: Description of global scale circulation cells in the Tropics with 40–50 day period. *J. Atmos. Sci.,* **29,** 1109–1123.

——, and ——, 1994: Observations of the 40–50-day tropical oscillation—A review. *Mon. Wea. Rev.,* **122,** 814–837.

Maloney, E. D., and D. L. Hartmann, 1998: Frictional moisture convergence in a composite life cycle of the Madden–Julian oscillation. *J. Climate,* **11,** 2387–2407.

——, and ——, 2000a: Modulation of eastern North Pacific hurricane activity in the Gulf of Mexico by the Madden–Julian oscillation. *Science,* **287,** 2002–2004.

——, and ——, 2000b: Modulation of eastern North Pacific hurricanes by the Madden–Julian oscillation. *J. Climate,* **13,** 1451–1460.

Mantua, N. J., S. R. Hare, Y. Zhang, J. M. Wallace, and R. C. Francis,

1997: A Pacific interdecadal climate oscillation with impacts on salmon production. *Bull. Amer. Meteor. Soc.,* **78,** 1069–1079.
Mo, K. C., and R. W. Higgins, 1998: Tropical convection and precipitation regimes in the western United States. *J. Climate,* **11,** 2404–2423.
Rui, H., and B. Wang, 1990: Development characteristics and dynamic structure of tropical intraseasonal convection anomalies. *J. Atmos. Sci.,* **47,** 357–379.
Schubert, S. D., and C.-K. Park, 1991: Low-frequency intraseasonal tropical extratropical interactions. *J. Atmos. Sci.,* **48,** 629–650.
Shinoda, T., H. H. Hendon, and J. Glick, 1998: Intraseasonal variability of surface fluxes and sea surface temperature in the tropical western Pacific and Indian Oceans. *J. Climate,* **11,** 1685–1702.
Vecchi, G. A., 2000: Tropical Pacific sub-seasonal wind variability and El Niño. Ph.D. dissertation, University of Washington, 187 pp.
——, and D. E. Harrison, 2000: Tropical Pacific sea surface temperature anomalies, El Niño, and equatorial westerly wind events. *J. Climate,* **13,** 1814–1830.
Waliser, D. E., C. Jones, J.-K. E. Schemm, and N. E. Graham, 1999: A statistical extended-range tropical forecast model based on the slow evolution of the Madden–Julian oscillation. *J. Climate,* **12,** 1918–1939.
——, K. M. Lau, W. Stern, and C. Jones, 2003: Potential predictability of the Madden–Julian oscillation. *Bull. Amer. Meteor. Soc.,* **84,** 33–50.
Wang, B., and X. Xie, 1998: Coupled models of the warm pool climate system. Part I: The role of air–sea interaction in maintaining Madden–Julian oscillation. *J. Climate,* **11,** 2116–2135.
Wheeler, M., and G. N. Kiladis, 1999: Convectively coupled equatorial waves: Analysis of clouds and temperature in the wavenumber-frequency domain. *J. Atmos. Sci.,* **56,** 374–399.
Widmann, M., and C. S. Bretherton, 2000: Validation of mesoscale precipitation in the NCEP reanalysis using a new gridcell dataset for the northwestern United States. *J. Climate,* **13,** 1936–1950.